




Article

Influence of TiO₂ Nanoparticles on the Resistance of Cementitious Composite Materials to the Action of Bacteria

Andreea Hegyi ¹, Adrian-Victor Lăzărescu ^{1,*} , Henriette Szilagyi ¹ , Elvira Grebenișan ¹, Jana Goia ² and Andreea Mircea ^{3,*} 

¹ NIRD URBAN-INCERC Cluj-Napoca Branch, 117 Calea Florești, 400524 Cluj-Napoca, Romania; andreea.hegyi@incerc-cluj.ro (A.H.); henriette.szilagyi@incerc-cluj.ro (H.S.); elvira.grebenisan@incerc-cluj.ro (E.G.)

² Municipal Hospital, 14–16 1 Mai Street, 405200 Dej, Romania; janagoia@yahoo.com

³ Facultatea de Construcții, Technical University of Cluj-Napoca, 28 Memorandumului, 400114 Cluj-Napoca, Romania

* Correspondence: adrian.lazarescu@incerc-cluj.ro (A.-V.L.); andreea.mircea@ccm.utcluj.ro (A.M.)

Abstract: The formation of biofilms on cementitious building surfaces can cause visible discoloration and premature deterioration, and it can also represent a potential health threat to building occupants. The use of embedded biofilm-resistant photoactivated TiO₂ nanoparticles at low concentrations in the cementitious composite matrix is an effective method to increase material durability and reduce maintenance costs. Zone of inhibition studies of TiO₂-infused cementitious samples showed efficacy toward both Gram-negative and Gram-positive bacteria.

Keywords: cementitious composites; TiO₂ nanoparticles; photocatalysis; bactericidal effect



Citation: Hegyi, A.; Lăzărescu, A.-V.; Szilagyi, H.; Grebenișan, E.; Goia, J.; Mircea, A. Influence of TiO₂ Nanoparticles on the Resistance of Cementitious Composite Materials to the Action of Bacteria. *Materials* **2021**, *14*, 1074. <https://doi.org/10.3390/ma14051074>

Academic Editor: Stefano Lettieri

Received: 20 January 2021

Accepted: 23 February 2021

Published: 25 February 2021

Publisher's Note: MDPI stays neutral with regard to jurisdictional claims in published maps and institutional affiliations.



Copyright: © 2021 by the authors. Licensee MDPI, Basel, Switzerland. This article is an open access article distributed under the terms and conditions of the Creative Commons Attribution (CC BY) license (<https://creativecommons.org/licenses/by/4.0/>).

1. Introduction

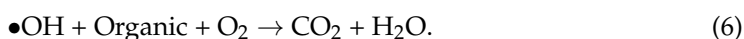
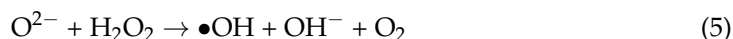
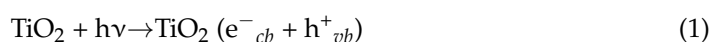
Worldwide, a shift in human lifestyles over the last half century has seen a growing number of daily activities move from the outdoors to enclosed inner spaces [1]. At the present time, it is known that the growth of micro-organisms (fungi, bacteria, viruses, algae, lichen, dust mites) on building surfaces (floors, walls, ceilings) has a detrimental effect on population health, particularly with contaminated interior surfaces. Maintaining good air quality and appearance of homes and workplaces has resulted in increased maintenance and repair costs. The existence of a so-called “Sick Building Syndrome (SBS)” manifests itself in the population that operates, partially or totally, inside buildings affected by mold or colonies (biofilms) of bacteria [1–3]. Pathogenic bacteria readily develop and survive on surfaces, especially in conditions of high humidity (min. 97%) and at temperatures ranging from –5 to +60 °C. The development of simple, inexpensive, and preventative antibacterial treatment methods of these surfaces are critical to maintain good public health [4,5]. In particular, areas of intensive medical use require the regular and thorough disinfection of surfaces in order to reduce the number of bacteria and prevent bacterial transmission to patients [4–7]. These untreated surfaces can act as reservoirs of microorganisms, which in turn could lead to the spread of infections [8]. Applications of the photocatalytic process of nano-TiO₂ provides a conceptually simple and promising preventative technology for inhibiting contamination from bacteria, as well as an alternative to the constant use of chemical disinfectants [5,9–11].

The specific properties of TiO₂ were discovered in the 1950s, but their exploitation in practical applications began only in 1972, when Fujishima and Honda used it for water splitting. Another very important property of TiO₂ is its photoinduced superhydrophilicity, which was unexpectedly discovered in 1995 in SiO₂/TiO₂ composites illuminated by ultraviolet (UV) light.

An important feature of TiO₂-SiO₂ compounds is that, unlike TiO₂, whose photocatalytic activity ceases without UV illumination, their photocatalytic effect continues for

hours or even days after the removal of the UV source. In 1997, the first publication by Luigi Cassar et al. focused on the production of cementitious materials with self-cleaning properties [12]. A significant amount of research has shown the benefits of the introduction of TiO₂ nanoparticles on the performance of cement composites: reduction of intake time, increase of the degree of cement hydration, increase of mechanical resistances (bending, compression, abrasion), adhesion to the reinforcement and resistance to its corrosion, and improvement of durability and freeze–thaw resistance [13–16].

In 1985, Matsunaga et al. first demonstrated the photocatalytic cytotoxic mechanisms in microbial cells from *Saccharomyces cerevisiae* (yeast), *Lactobacillus acidophilus* and *Escherichia coli* (bacteria), and *Chlorella vulgaris* (green algae) in water [17–21]. It is currently known that when the supplied photon energy is greater than the energy difference between the valence and conduction band edges of TiO₂ (which occurs for UV radiation), photogenerated electrons (e[−]) and holes (h⁺) react with O₂ and H₂O, forming anionic radicals (O^{2−}) and (OH). These oxidative species (h⁺, O^{2−}, and OH) are highly reactive, contributing to the destruction of the cells of microorganisms [1,22–26]. The mechanism of destruction can be synthesized in the following sequence of reactions:



A number of studies have been carried out in this direction. Sunada et al. [27] have shown that cell membranes are photocatalytically destroyed in the case of *Escherichia coli* bacteria. Saito et al. [28] proposed a mechanism for the destruction of bacteria by inhibiting their respiration function once they come into contact with TiO₂. Oguma et al. [29] discussed a mechanism for the destruction of bacteria through the destruction of the cell wall and the induction of disorder at the cellular level following the contact of the microorganism with TiO₂. Evidences highlight that wavelengths in the range of 320–400 nm are the most efficient to activate the photo-cytotoxic activity of TiO₂. Gogniat et al. [30] showed that the adsorption capacity of TiO₂ is positively correlated with its biocidal effect. Adsorption has been consistently associated with a reduction in the integrity of the bacterial membrane, as indicated by flow cytometry. The authors suggested that the adsorption of cells on photoactivated TiO₂ is followed by a loss of membrane integrity, which was key to the biocidal effect. Mazurkova et al. [31] analyzed the effect of nano-TiO₂ on the influenza virus, indicating the destruction of the virus in the presence of nanoparticles. After 15 min of incubation, the nanoparticles adhered to the outer surface of the virus, the surface spinules of the virus were glued together, and its outer membrane, of a lipoprotein nature, was torn. After 30 min, the degree of destruction increased, and after 1–5 h of incubation, the virus that came into contact with the nanoparticles was completely destroyed. It is considered that this effect depends on the duration of exposure/incubation, the viral concentration, and the concentration of nano-TiO₂. The tests were carried out in three lighting conditions: dark, UV radiation, and natural light. Adams et al. [32] showed that the concentration of *Bacillus subtilis* and *Escherichia coli* were reduced upon contact with a suspension of nano-TiO₂ under natural light illumination. A similar effect on *Bacillus subtilis* has been reported by Armelao et al. [33]. Research conducted by Dedkova et al. [34] on samples of kaolin composites containing nano-TiO₂ indicated their biocidal effect in the presence of *Escherichia coli*, *Enterococcus faecalis*, and *Pseudomonas Aeruginosa*, after 2 days of exposure to artificial light. Results were also consistent with those of Gurr [35], who assessed that the antibacterial effect of TiO₂ composites is manifested in the presence of

natural light, without necessarily requiring UV photoactivation. The study carried out by Hamdani [36] has shown that based on the behavior of the two cementitious mixtures with 3% and 5% nano-TiO₂-based type-Aeroxide P25, when in contact with *E. coli*, they were able to reduce the viability of bacteria after 24 h of exposure by 60–70%. The main observation, based on results in the literature [37–39], is that cementitious composite surfaces containing nano-TiO₂ have the ability to inhibit biofilm growth, destroying the *E-coli bacteria* with which they come in contact. This is also supported by results obtained by Daly et al. [40], Carre et al. [41], and Kubacka et al. [42], which confirm that by the formation of free radicals and anions strongly oxidized by the photoactivation of nano-TiO₂ (OH• and O₂[−]), at the cellular level, plasma components such as DNA, RNA, lipids, and proteins are destroyed, and cell membranes are broken.

The easiest method of studying the resistance capacity of various building materials to the attack of microorganisms is the adapted antibiogram method, which is already used in medicine. This method is known as the halo inhibition method [43] or the Kirby–Bauer method, and it is currently standardized according to AATCC TM147 and AATCC TM30 (American Association of Textile Chemists and Colorists).

Although a large number of authors confirm the anti-bactericidal capacity of cement compounds with nano-TiO₂, there is still controversy about maintaining the bactericidal capacity in the absence of light (during the night), as well as the influence of the type of bacteria that contaminate the surface. Results show that their destruction begins after only 20 min of UV radiation exposure and 60–120 min is sufficient to destroy all the bacteria [44], since hydroxyl radicals are the main factors responsible for the bactericidal capacity of semiconductor's photocatalysts. They also possess a destruction capacity of *Escherichia coli* bacteria which is 10³–10⁴ times more effective than chemical disinfection products [45].

The aim of this work is to analyze the potential of inhibiting the growth of bacterial films on the surface of cementitious composites by adding different amounts of nano-TiO₂, using the zone of inhibition to get a quick test of the antibacterial efficiency, and to identify the nanoparticle-functionalized regions in relation to the amount of cement, which ensure a successful effect of resistance from a biological point of view. For this purpose, four types of bacteria were used, which were chosen because of the frequency with which they are encountered in the building environment: *Escherichia coli*, *Pseudomonas Aeruginosa*, *Staphylococcus Aureus*, and *Streptococcus Pyogenes*.

2. Materials and Methods

In order to study the self-cleaning and anti-bacterial properties of cementitious composites, the literature shows three types of concrete modifications: concrete covered with a thin layer of TiO₂, concrete covered by a thick layer of photoactive concrete on the top, and finally, different weight percentages of TiO₂ in the concrete mass (when TiO₂ substitutes cement or is present as additive) [46]. Each of these approaches has advantages and disadvantages in relation to the compatibility and adhesion to the substrate (in the case of thin films on the surface), durability, and impact on physical and mechanical performances (in the case of the introduction of TiO₂ nanoparticles into the cementitious mass) and even economic impact in terms of costs [47]. The methodology used was based on the studies presented by Meija-De Gutierrez [43].

The preparation of the cementitious composites was performed by using white Portland cement as binder and by adding TiO₂ nanoparticles as addition in different mass percentages, relative to cement quantity. Preliminary results obtained on the same mix-design ratios, when subjected to the method of staining with Rhodamine B and methylene blue, extended even for the situation of staining with exhaustion gas particles on the surface of the samples [48,49], have demonstrated the photocatalytic activity of nano-TiO₂ addition in the cementitious matrix and thus the self-cleaning capacity of the samples. Furthermore, the influence of added TiO₂ nanoparticles on the hydrophilicity of the cementitious composites surfaces was studied on the same mixtures [50].

Commercial Aeroxide P25 TiO₂ nanoparticles, 99.5% purity (Evonik Industries AG, Hanau, Germany), containing more than 70% anatase, with a minor amount of rutile and a small amount of amorphous phase anatase and rutile crystallites, with a reported ratio of 70:30 or 80:20, were used in the production of the samples. Both phases play an important role in industrial applications and contribute to the photoactivation mechanism [3]. According to the manufacturer's data sheet, the mean size of the TiO₂ particles is 21 nm, with a specific surface of 35–65 m²/g. The test specimens were prepared and conditioned as shown in Table 1 in order to conduct the specific tests.

Table 1. Mix ratio and conditioning of cementitious composites.

Mixture Number	P1	P2	P3	P4	P5	P6	P7	P8	P9	P10
Amount of nanoparticles relative to the amount of cement (%)	0	1	2	3	3.6	4	5	6	10	12
CEM I 52,5R white cement, HOLCIM (g)	500	500	500	500	500	500	500	500	500	500
Amount of water relative to the amount of total dry mixture (water/(cement + nano-TiO ₂)) (g)	0.5									
Conditioning	<ul style="list-style-type: none"> - 24 h in molds, 90% RH, 20 °C, without light; - demolding; - 27 days complete water immersion, 20 °C, without light. 									

Then, the cementitious composite paste was cast into rectangular molds from which small, 17.4 mm circular samples were cut. Then, the samples were subjected to photoactivation, undergoing a 24 h UV ray treatment by using a light source with 400–315 nm spectrum emission (corresponding to the UVA band), which was located at a distance of 10 cm above the surface of the specimens, which determined a luminous flux intensity of 860 lux.

For testing resistance to the action of bacteria of the nano-TiO₂ cementitious composite samples, *Escherichia coli* (ATCC 25922), *Pseudomonas Aeruginosa* (ATCC 27853), *Staphylococcus Aureus* (ATCC 25923), and *Streptococcus Pyogenes* (ATCC 19615) solutions have been used. These solutions were prepared by harvesting them from reference bacteria cultures and introducing 2 colonies (2 loops of 1 µL each) of biological material into 1 mL of physiological serum. The biological load of the prepared solutions was semi-quantified by the contact plate method, using the specifications of MicroKount[®] microbiologic load test (Figure 1), determining a concentration of 10⁷ CFUs for each type of bacteria used.

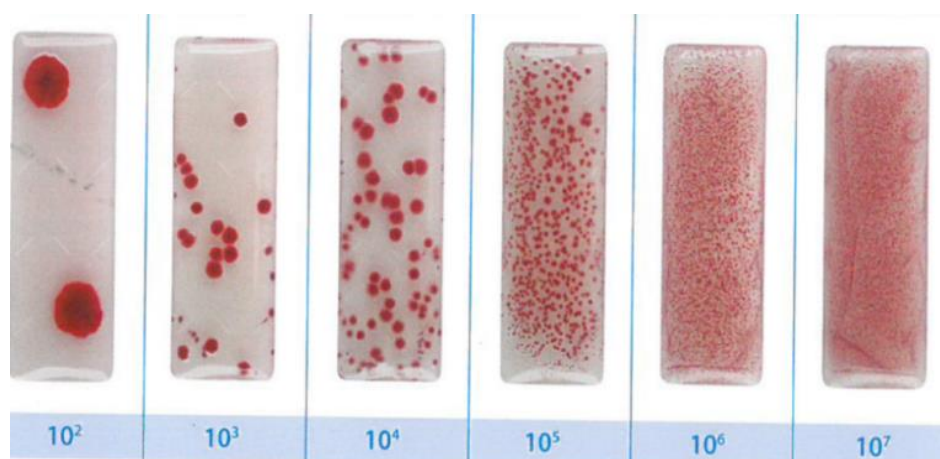


Figure 1. Quantification of biological load according to MicroKount[®] specifications.

At the same time, $\varphi = 90$ mm Petri dishes were prepared, in which suitable nutrient substrates were placed in order to develop the bacteria cultures, such as agar for bacteria cultures *Escherichia coli*, *Pseudomonas Aeruginosa*, and *Staphylococcus Aureus*, respectively, and blood agar for bacteria culture *Streptococcus Pyogenes*. All of them were sterilized under UV rays.

In each sterilized Petri dish with a suitable nutrient substrate, depending on the type of bacteria, 1 mL of bacterium suspension was applied and distributed so that the entire surface of the nutrient substrate was covered. Consequently, the photoactivated cementitious composite samples were centrally placed in the Petri dishes without any cross-contamination of the system.

Subsequently, 0.5 mL of biological material–bacterium suspension was applied on the samples, and the Petri dish lid was sealed by isolating the whole system on the edge to prevent cross contamination. One sample for each type of bacteria used was made without using any cementitious composite sample (P0). This was considered the primary control sample and was used to demonstrate the viability of the used bacteria in the suspensions.

Romanian STAS 12718 offers the possibility of semi-quantitative quantification of the microbiological load of the system, providing a quantification grid as follows: 0 (–) no growth (sterile); 1 (+) 1–10 colonies of microorganisms; 2 (++) over 10 colonies of microorganisms; 3 (+++) areas with confluent colonies; 4 (++++) growth throughout the surface.

Then, the farming systems were placed in the laboratory, at a temperature of 30 °C, under natural light conditions. As a result of exposure to natural light, the photoactivation process initially induced by UV exposure was continuously refreshed throughout 21 days, similarly to the alternation of day/night periods. Moreover, the initial UV exposure, for 24 h, ensured the sterilization of the cementitious samples so that there was no pre-existing contamination. At regular intervals of time, i.e., 2, 3, 4, 6, 7, 14, and 21 days, the development of the systems was examined visually and microscopically for signs of growth/development of the material (the colonies). The presence/development of the halo of inhibition was also studied. The quantification of the behavior of the bacteria contaminated samples was carried out qualitatively, according to STAS 12718 (Table 2) and using the Kirby–Bauer technique (AATCC TMII47), which is commonly used in medicine and has been known since 1966 as the antibiogram method. This method was adapted to the present requirements and conditions, by which the diameter of the inhibition halo, φ (mm) was measured.

Table 2. Quantification of the biological load according to STAS 12718.

0 (–)	no growth (sterile)
1 (+)	1–10 colonies of microorganisms
2 (++)	over 10 colonies of microorganisms
3 (+++)	areas with confluent colonies
4 (++++)	growth throughout the surface

The effectiveness of the antibacterial effect induced by nano-TiO₂ photoactivation was assessed quantitatively by introducing a quantifiable parameter, EEA, which represents the percentage change in the diameter of the inhibition halo of the analyzed sample (with nano-TiO₂ content in the matrix >0, relative to the control sample (with 0% nano-TiO₂ content in the matrix), according to Equation (7).

$$EEA = (\varphi_{\%TiO_2} - \varphi_{control}) / \varphi_{control} \times 100 (\%) \quad (7)$$

where $\varphi_{\%TiO_2}$ —inhibition halo diameter measured for the sample with TiO₂% > 0 (mm); $\varphi_{control}$ —inhibition halo diameter measured for TiO₂ 0% control sample (mm).

3. Results and Discussion

Experimental results on the behavior of cementitious composites with the addition of TiO₂ in an environment contaminated with *Escherichia coli* are presented in Table 3 and in Figures 2 and 3. For the environment contaminated with *Pseudomonas Aeruginosa*, results are presented in Table 4 and in Figures 3 and 4. For the environment contaminated with *Staphylococcus Aureus*, results are shown in Table 5 and in Figures 3 and 5 and for the samples contaminated with *Streptococcus Pyogenes*, results are shown in Table 6 and in Figures 3 and 6.

Table 3. Quantification of the microbiological load of the system according to STAS 12718 for samples exposed to *Escherichia coli*.

Exposure Period (Days)	P0 (without Composite Sample)	P1 (0% TiO ₂)	P2 (1% TiO ₂)	P3 (2% TiO ₂)	P4 (3% TiO ₂)	P5 (3.6% TiO ₂)	P6 (4% TiO ₂)	P7 (5% TiO ₂)	P8 (6% TiO ₂)	P10 (12% TiO ₂)
2	1 (+)	1 (+)	1 (+)	1 (+)	1 (+)	1 (+)	0 (-)	0 (-)	0 (-)	0 (-)
3	1 (+)	1 (+)	1 (+)	1 (+)	1 (+)	1 (+)	0 (-)	0 (-)	0 (-)	0 (-)
4	3 (+++)	1 (+)	1 (+)	1 (+)	1 (+)	1 (+)	0 (-)	0 (-)	0 (-)	0 (-)
6	3 (+++)	1 (+)	1 (+)	1 (+)	1 (+)	1 (+)	0 (-)	0 (-)	1 (+)	1 (+)
7	3 (+++)	1 (+)	1 (+)	1 (+)	1 (+)	1 (+)	0 (-)	1 (+)	1 (+)	1 (+)
14	3 (+++)	1 (+)	1 (+)	1 (+)	1 (+)	1 (+)	1 (+)	1 (+)	1 (+)	1 (+)
21	3 (+++)	1 (+)	3 (+++)	1 (+)	3 (+++)	3 (+++)	2 (++)	1 (+)	1 (+)	1 (+)

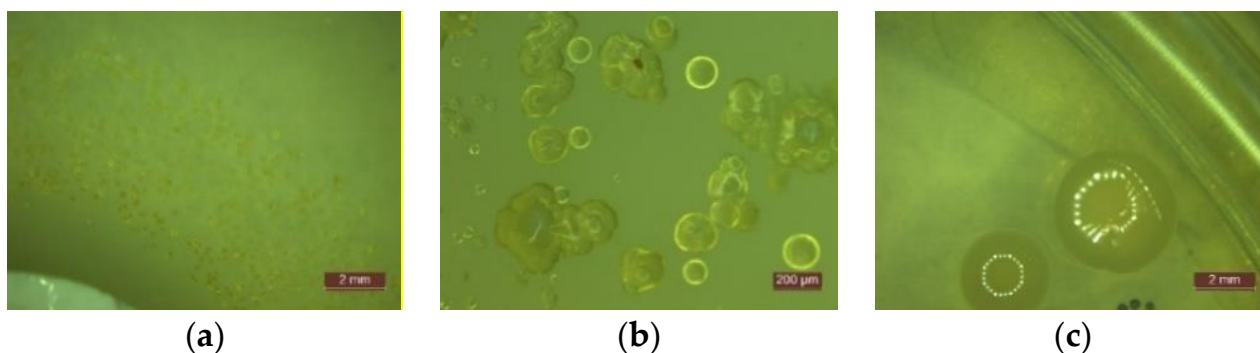


Figure 2. Microscopic examination of the behavior of samples exposed to *Escherichia coli*: (a) Identification of the inhibition halo area (1:2 mm); (b) Growth colonies (1:200 μm); (c) Detail of growth colonies (1:2 mm).

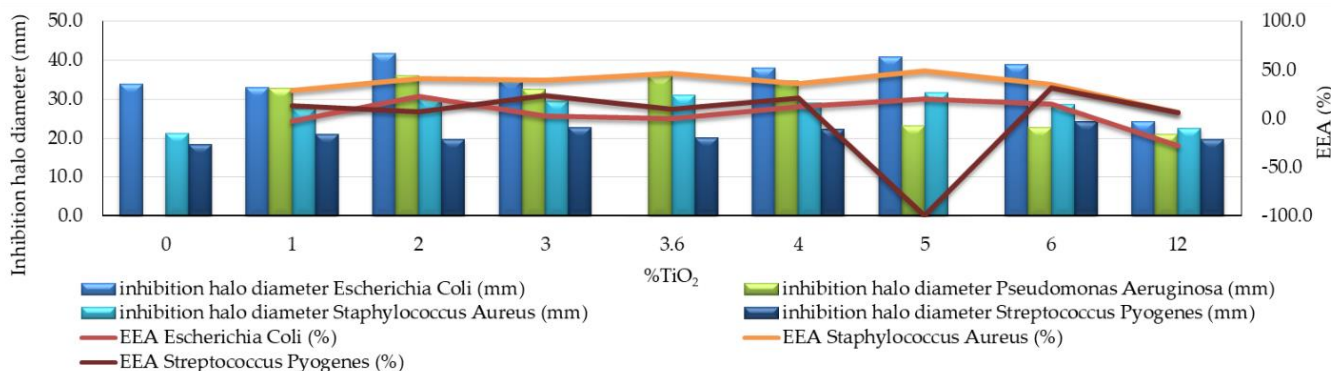
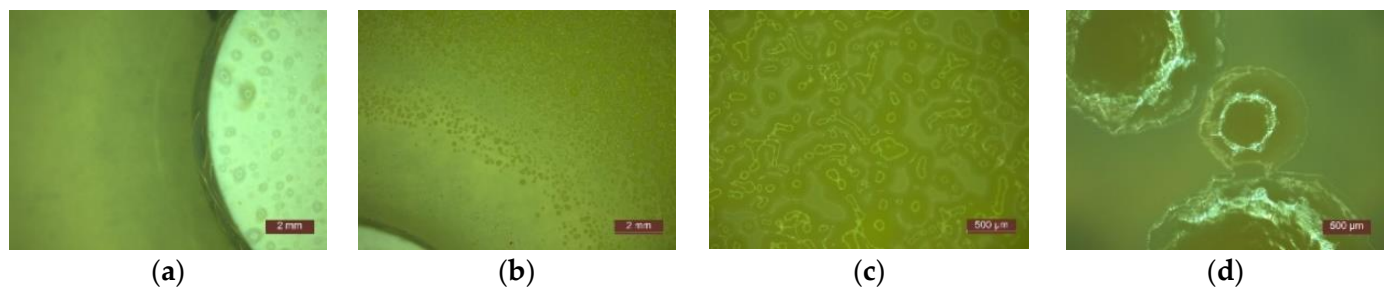


Figure 3. Inhibition halo size development after 2 days of exposure to bacteria *Escherichia coli*, *Pseudomonas Aeruginosa*, *Staphylococcus Aureus*, and *Streptococcus Pyogenes*. (In the case of *Pseudomonas Aeruginosa* contamination, the EEA could not be quantified, because the control sample (0% TiO₂) did not show an inhibition halo). EEA: the percentage change in the diameter of the inhibition halo of the analyzed sample, indicating the effectiveness of the antibacterial effect.

Table 4. Quantification of the microbiological load of the system according to STAS 12718 for samples exposed to *Pseudomonas Aeruginosa*.

Exposure Period (Days)	P0 (Without Composite Sample)	P1 (0% TiO ₂)	P2 (1% TiO ₂)	P3 (2% TiO ₂)	P4 (3% TiO ₂)	P5 (3.6% TiO ₂)	P6 (4% TiO ₂)	P7 (5% TiO ₂)	P8 (6% TiO ₂)	P10 (12% TiO ₂)
2	3 (+++)	3 (+++)	2 (++)	2 (++)	2 (++)	2 (++)	2 (++)	2 (++)	2 (++)	2 (++)
3	3 (+++)	3 (+++)	2 (++)	2 (++)	2 (++)	2 (++)	2 (++)	2 (++)	2 (++)	2 (++)
4	3 (+++)	3 (+++)	2 (++)	2 (++)	2 (++)	2 (++)	2 (++)	2 (++)	2 (++)	2 (++)
6	3 (+++)	3 (+++)	2 (++)	2 (++)	2 (++)	2 (++)	2 (++)	2 (++)	2 (++)	2 (++)
7	3 (+++)	3 (+++)	3 (+++)	2 (++)	2 (++)	2 (++)	2 (++)	2 (++)	2 (++)	2 (++)
14	3 (+++)	3 (+++)	3 (+++)	3 (+++)	2 (++)	2 (++)	2 (++)	2 (++)	2 (++)	2 (++)
21	3 (+++)	3 (+++)	3 (+++)	3 (+++)	3 (+++)	2 (++)	2 (++)	2 (++)	2 (++)	2 (++)

**Figure 4.** Microscopic examination of the behavior of samples exposed to *Pseudomonas Aeruginosa*: (a) The presence of biological material on the surface of the composite specimen at the time of sowing (1:2 mm); (b) Identification of the inhibition halo zone (1:2 mm); (c) Growth of colonies (1:500 μm); (d) Detail growth of colonies (1:500 μm).**Table 5.** Quantification of the microbiological load of the system according to STAS 12718 for samples exposed to *Staphylococcus Aureus*.

Exposure Period (Days)	P0 (without Composite Sample)	P1 (0% TiO ₂)	P2 (1% TiO ₂)	P3 (2% TiO ₂)	P4 (3% TiO ₂)	P5 (3.6% TiO ₂)	P6 (4% TiO ₂)	P7 (5% TiO ₂)	P8 (6% TiO ₂)	P10 (12% TiO ₂)
2	0 (-)	0 (-)	0 (-)	0 (-)	0 (-)	0 (-)	0 (-)	0 (-)	0 (-)	0 (-)
3	1 (+)	1 (+)	0 (-)	0 (-)	0 (-)	0 (-)	0 (-)	1 (+)	0 (-)	0 (-)
4	1 (+)	1 (+)	0 (-)	0 (-)	1 (+)	0 (-)	0 (-)	1 (+)	0 (-)	1 (+)
6	1 (+)	1 (+)	1 (+)	0 (-)	1 (+)	0 (-)	1 (+)	1 (+)	0 (-)	1 (+)
7	1 (+)	1 (+)	1 (+)	0 (-)	1 (+)	1 (+)	1 (+)	3 (+++)	0 (-)	1 (+)
14	1 (+)	1 (+)	1 (+)	0 (-)	1 (+)	1 (+)	1 (+)	3 (+++)	1 (+)	1 (+)
21	1 (+)	1 (+)	1 (+)	1 (+)	1 (+)	1 (+)	1 (+)	3 (+++)	1 (+)	1 (+)

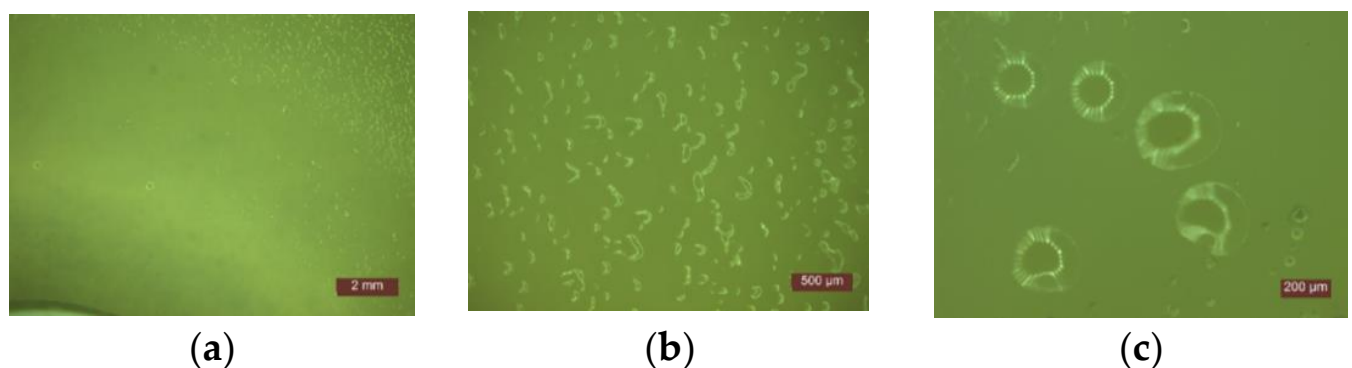
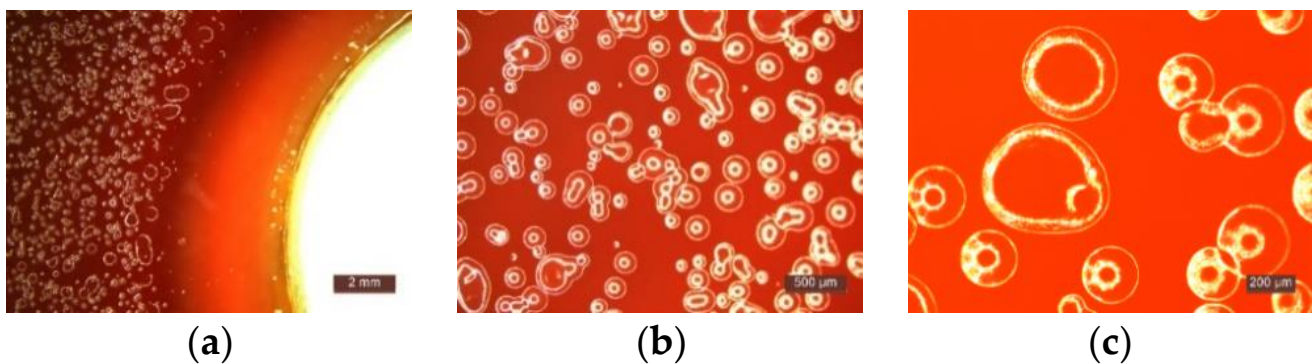
**Figure 5.** Microscopic examination of the behavior of samples exposed to *Staphylococcus Aureus*: (a) Identification of the inhibition halo area (1:2 mm); (b) Growth of colonies (1:500 μm); (c) Detail growth of colonies (1:200 μm).

Table 6. Quantification of the microbiological load of the system according to STAS 12718 for samples exposed to *Streptococcus Pyogenes*.

Exposure Period (Days)	P0 (without Composite Sample)	P1 (0% TiO ₂)	P2 (1% TiO ₂)	P3 (2% TiO ₂)	P4 (3% TiO ₂)	P5 (3.6% TiO ₂)	P6 (4% TiO ₂)	P7 (5% TiO ₂)	P8 (6% TiO ₂)	P10 (12% TiO ₂)
2	2 (++)	2 (++)	1 (+)	1 (+)	1 (+)	1 (+)	1 (+)	1 (+)	1 (+)	2 (++)
3	3 (+++)	2 (++)	2 (++)	1 (+)	1 (+)	1 (+)	1 (+)	1 (+)	1 (+)	2 (++)
4	3 (+++)	2 (++)	2 (++)	2 (++)	2 (++)	2 (++)	2 (++)	2 (++)	2 (++)	2 (++)
6	3 (+++)	3 (+++)	3 (+++)	2 (++)	2 (++)	2 (++)	2 (++)	2 (++)	3 (+++)	3 (+++)
7	3 (+++)	3 (+++)	3 (+++)	2 (++)	2 (++)	2 (++)	2 (++)	3 (+++)	3 (+++)	3 (+++)
14	4 (++++)	4 (++++)	3 (+++)	3 (+++)	3 (+++)	3 (+++)	3 (+++)	3 (+++)	4 (++++)	4 (++++)
21	4 (++++)	4 (++++)	4 (++++)	3 (+++)	3 (+++)	3 (+++)	3 (+++)	3 (+++)	4 (++++)	4 (++++)

**Figure 6.** Microscopic examination of the behavior of samples exposed to *Streptococcus Pyogenes*: (a) Identification of the inhibition halo area (1:2 mm); (b) Growth of colonies (1:500 μm); (c) Detail growth of colonies (1:200 μm).

By analyzing the obtained results, several general features have been observed on all systems, regardless of the type of contaminant:

- No traces of contamination/development of bacterial colonies were observed on the surface of any of the tested cementitious material samples during the entire test period (21 days).
- In the first 48 h after exposure in the contaminated environment, the formation of inhibition haloes was observed, which remained constant in size and shape throughout the test. The systems presented a concentric shape: the cementitious composite sample being surrounded by a circular area with microbiological load, evaluated according to STAS 12718/1989, in Class 0 (-). This was followed by a zone of growth and the development of biological material. This increase was more intense as the distance from the edge of the cementitious composite increased (Figures 2–7). The only exception was observed for samples tested with *Pseudomonas Aeruginosa*, for which no inhibition halo was identified in the cementitious composite control system.
- Sample P10 (12% TiO₂) had in general a smaller halo diameter than samples with lower nanoparticle content. This behavior can be attributed to the inhomogeneity and the improper dispersion of nanoparticles in the cementitious matrix, which may tend to agglomerate.
- The P0 system, without the cementitious composite sample, had the most intense and rapid development of colonies of bacteria.
- Microscopic analysis revealed the presence and development of colonies of bacteria in the areas outside the inhibition halo, which again indicate the viability of the suspension used for seeding, the right choice of nutrient substrate, and exposure conditions.
- The formation of the inhibition halo for the control composite system (0% TiO₂) also indicated resistance to the development of bacteria. This mainly happened because of the chemical composition of white Portland cement, which usually contains a certain quantity of TiO₂.

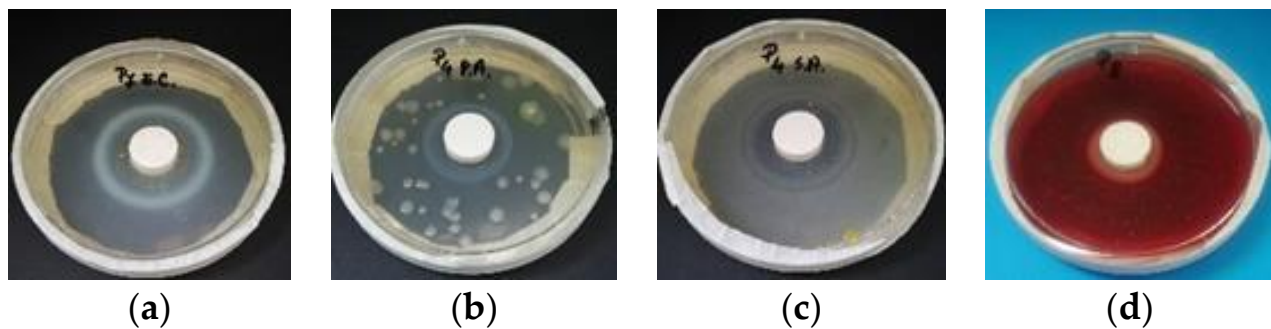


Figure 7. Nano-TiO₂ systems evaluation: (a) 5% TiO₂, (14 days exposure to *Escherichia coli*); (b) 3.6% TiO₂ (6 days exposure to *Pseudomonas Aeruginosa*); (c) 3% TiO₂ (14 days exposure to *Staphylococcus Aureus*); (d) 6% TiO₂ (21 days exposure to *Streptococcus Pyogenes*).

In case of contamination with *Escherichia coli*, the following aspects could be identified:

- Cementitious composites with nano-TiO₂ content in the range of 2–6% had the most effective behavior, with an efficiency of the antibacterial effect (EEA) of more than 10% (Figure 3). The highest value of this parameter (23%) was reported for the samples with 2% nano-TiO₂ addition.
- When evaluating the entire system by quantifying the microbiological load of the system, according to STAS 12718 (Table 3), Classes 0 (-) or 1 (+) were observed/maintained for a longer period. It was also noticed that the samples with 4–12% nano-TiO₂—(Class 0 (-))—maintain this sterile behavior longer (even after 7 days of exposure in contaminated environment—sample P6 (4% TiO₂)). In addition, the P3 sample (2% TiO₂) had a distinguished behavior, by keeping Class 1 (+) constant until the end of the test period.
- In the case of the P0 system, the formation of zones with confluent colonies (Class 3 (+++)) was observed earlier, after only 4 days at exposure in the contaminated environment. This confirmed the viability of the inoculated bacterial material.

In the case of contamination with *Pseudomonas Aeruginosa*, the following aspects can be identified:

- Due to the lack of visible and measurable inhibition halo in the control sample, the effectiveness of the antibacterial effect (EEA) could not be calculated, thus indicating a resistance effect to these bacteria of the cementitious composite matrix (Figure 3). However, for samples with 3.6% and 4% nano-TiO₂, large inhibition halos have been observed.
- When evaluating the entire system by quantifying the microbiological load of the system, according to STAS 12718 (Table 4), Class 2 (++) was observed and maintained for a longer period. This happened due to the higher content of nanoparticles in the cementitious composite mass. For composite samples with 3.6–12% nano-TiO₂, the framing Class 2 (++) was maintained throughout the 21 days of testing. This also happened for sample P4 (3% TiO₂), whose framing class changed from 2 (++) to 3 (+++) only at the last stage of testing (during 14–21 days of exposure in the contaminated environment).
- In the case of the P0 system and the P1 control sample system (0% TiO₂), the formation of areas with Class 3 (+++) confluent colonies was rapidly observed after 2 days of exposure in the contaminated environment, which on the one hand indicates the pre-viability of the bacterial inoculum material and on the other hand indicates the lack of antibacterial activity in the case of the P1 control composite matrix (0% TiO₂) (Table 4).

In the case of contamination with *Staphylococcus Aureus*, the following aspects could be identified:

- Samples containing nano-TiO₂ in the range of 1% to 5% had the most satisfactory behavior, i.e., an efficiency of the antibacterial effect (EEA) of more than 25% (Figure 3). The maximum effectiveness of the antibacterial effect (EEA) was achieved by the samples with 5% nano-TiO₂, for which this indicator was 49%.
- The development of *Staphylococcus Aureus* colonies occurred less readily compared to the other types of bacteria analyzed in the study. The identified colonies were visible to the naked eye after only 2–3 days of exposure in the contaminated environment.
- In the case of the P0 system, colony formation Class 1 (+) was observed after 3 days of exposure, which confirms the viability of the inoculated bacterial material (Table 5).

In the case of contamination with *Streptococcus Pyogenes*, the following aspects could be identified:

- Samples with nano-TiO₂ content in the range of 3–6% showed better behavior in terms of the ability to inhibit colony growth.
- When evaluating the entire system by quantifying the microbiological load of the system, according to STAS 12718 (Table 6), Classes 1 (+) or 2 (++) were observed and maintained during the first 2–3 days after exposure to the contaminated environment. For samples with 2–6% nano-TiO₂, this classification was kept constant for up to 3 days. In these cases, the EEA quantifiable parameter reached the maximum value, i.e., 31%, for the 6% nano-TiO₂ composition (Figure 3);
- In the case of the P0 system, the formation of more than 10 colonies, Class 2 (++) was observed after 2 days, Class 3 (+++) confluent colonies were observed after 3 days, and also Class 4 (++++) growth was observed throughout the surface (Table 6). Almost the same behavior, differentiated only by the delay in their development, was observed for P1 (0% TiO₂), P2 (1% TiO₂), and even the system with the maximum nanoparticle content, P10 (12% TiO₂).

4. Conclusions

From the research performed, we can draw the following conclusions:

- The viability of the contaminants, selection of nutrients, and temperature conditions were proven. Therefore, the identification, quantification, and comparison between their action and the results regarding the growth of the biological material, when subjected to the cementitious composites, was demonstrated, based on the retention time of the samples in the contaminated environment and the content of nano-TiO₂ in the samples.
- The effect of the development of the inhibition halo, when subjected to *Escherichia coli*, *Pseudomonas Aeruginosa*, and *Staphylococcus Aureus* bacteria, namely, *Streptococcus Pyogenes* has also been confirmed for samples containing nano-TiO₂ in the range of 2% to 5%. However, the introduction of large quantities of nanoparticles in the matrix of the composite may be on one hand beneficial in terms of antibacterial effects but, on the other hand, it is harmful as a result of the tendency of agglomeration of the nanoparticles in the matrix of the composite. Therefore, the effect of the antibacterial agent is considerably reduced.
- It was considered that for a good inhibiting activity against the development of contaminants of type *Escherichia coli*, *Pseudomonas Aeruginosa*, *Staphylococcus Aureus*, and *Streptococcus Pyogenes*, the content of TiO₂ nanoparticles in the cementitious composite matrix should be at least 2% and not more than 5% relative to the amount of cement. The possibility remains open that composite samples with more than 5% nano-TiO₂ are antibacterial effective if adequate nanoparticle dispersion is ensured. This range of identified nano-TiO₂ amount is consistent with reports in the literature [36–42,51–56].

The results and observations presented in this paper can be a starting point for further research, consisting of a relatively fast and inexpensive semi-quantitative method for evaluating the antibacterial performance of cementitious composites with nano-TiO₂. Through the work process adopted, it was also possible to highlight the antibacterial

efficiency of cementitious composites with different nano-TiO₂ percentages and to open new perspectives in the development of self-cleaning construction materials.

Author Contributions: Conceptualization, A.H., A.M. and H.S.; methodology, E.G. and J.G.; validation, A.H., H.S., A.-V.L. and A.M.; investigation, A.H., E.G., J.G. and A.-V.L.; resources, H.S., J.G. and A.M.; data curation, A.H., E.G., H.S. and A.-V.L.; writing—original draft preparation, A.H.; writing—review and editing, A.H., E.G., H.S. and A.-V.L.; visualization, A.-V.L.; supervision, A.H., H.S., A.M. All authors have read and agreed to the published version of the manuscript.

Funding: This research received no external funding.

Institutional Review Board Statement: Not applicable.

Informed Consent Statement: Not applicable.

Data Availability Statement: The data presented in this study are available on request from the corresponding authors.

Acknowledgments: The authors would like to thank Michael Grantham of Sandberg LLP (former Visiting Professor at The University of Leeds and Queen's University Belfast and a Past President of the Institute of Concrete Technology, UK) for his support and contribution in technical editing, language editing and proofreading.

Conflicts of Interest: The authors declare no conflict of interest.

References

1. Haleem Khan, A.A.; Mohan Karuppaiyil, S. Fungal pollution of indoor environments and its management. *Saudi J. Biol. Sci.* **2012**, *19*, 405–426. [\[CrossRef\]](#)
2. Ebbehøj, N.E.; Hansen, M.O.; Sigsgaard, T.; Larsen, L. Building-related symptoms and molds: A two-step intervention study. *Indoor Air* **2002**, *12*, 273–277. [\[CrossRef\]](#)
3. Zeliger, H.I. Toxic effects of chemical mixtures. *Arch. Environ. Health* **2003**, *58*, 23–29. [\[CrossRef\]](#)
4. Yadav, H.M.; Kim, J.S.; Pawar, S.H. Developments in photocatalytic antibacterial activity of nano TiO₂: A review. *Korean J. Chem. Eng.* **2016**, *33*, 1989–1998. [\[CrossRef\]](#)
5. Wang, L.; Hu, C.; Shao, L. The antimicrobial activity of nanoparticles: Present situation and prospects for the future. *Int. J. Nanomed.* **2017**, *12*, 1227–1249. [\[CrossRef\]](#)
6. Kühn, K.P.; Chaberny, I.F.; Massholder, K.; Stickler, M.; Benz, V.W.; Sonntag, H.G.; Erdinger, L. Disinfection of surfaces by photocatalytic oxidation with titanium dioxide and UVA light. *Chemosphere* **2003**, *53*, 71–77. [\[CrossRef\]](#)
7. Drugă, B.; Ukrainczyk, N.; Weise, K.; Koenders, E.; Lackner, S. Interaction between wastewater microorganisms and geopolymer or cementitious materials: Biofilm characterization and deterioration characteristics of mortars. *Int. Biodeterior. Biodegrad.* **2018**, *134*, 58–67. [\[CrossRef\]](#)
8. Machida, M.; Norimoto, K.; Kimura, T. Antibacterial Activity of Photocatalytic Titanium Dioxide Thin Films with Photodeposited Silver on the Surface of Sanitary Ware. *J. Am. Ceram. Soc.* **2005**, *88*, 95–100. [\[CrossRef\]](#)
9. Page, K.; Wilson, M.; Parkin, I.P. Antimicrobial surfaces and their potential in reducing the role of the inanimate environment in the incidence of hospital-acquired infections. *J. Mater. Chem.* **2009**, *19*, 3819. [\[CrossRef\]](#)
10. Watts, R.J.; Kong, S.; Orr, M.P.; Miller, G.C.; Henry, B.E. Photocatalytic inactivation of coliform bacteria and viruses in secondary wastewater effluent. *Water Res.* **1995**, *29*, 95–100. [\[CrossRef\]](#)
11. Vohra, A.; Goswami, D.Y.; Deshpande, D.A.; Block, S.S. Enhanced photocatalytic inactivation of bacterial spores on surfaces in air. *J. Ind. Microbiol. Biotechnol.* **2005**, *32*, 364–370. [\[CrossRef\]](#)
12. Cassar, L. Nanotechnology and photocatalysis in cementitious materials. In *NICOM 2: 2nd International Symposium on Nanotechnology in Construction*; de Miguel, Y., Porro, A., Bartos, P.J.M., Eds.; RILEM Publications SARL: Paris, France, 2006; pp. 277–284.
13. Wang, L.; Zhang, H.; Gao, Y. Effect of TiO₂ nanoparticles on physical and mechanical properties of cement at low temperatures. *Adv. Mater. Sci. Eng.* **2018**, *2018*, 8934689. [\[CrossRef\]](#)
14. Sadawy, M.M.; Elsharkawy, E.R. Effect of Nano-TiO₂ on mechanical properties of concrete and corrosion behavior of reinforcement bars. *Int. J. Eng. Res. Appl.* **2016**, *6*, 61–65.
15. Salemi, N.; Behfarnia, K.; Zaree, S.A. Effect of nanoparticles on frost durability of concrete. *Asian J. Civ. Eng.* **2014**, *15*, 411–420.
16. Shen, W.; Zhang, C.; Li, Q.; Zhang, W.; Cao, L.; Ye, J. Preparation of titanium dioxide nano particle modified photocatalytic self-cleaning concrete. *J. Clean. Prod.* **2015**, *87*, 762–765. [\[CrossRef\]](#)
17. Matsunaga, T.; Tomoda, R.; Nakajima, T.; Nakamura, N.; Komine, T. Continuous-sterilization system that uses photoconductor powders. *Appl. Environ. Microbiol.* **1988**, *54*, 1330–1333. [\[CrossRef\]](#)
18. Abdel-Gawwad, H.A.; Mohamed, S.A.; Mohammed, M.S. Recycling of slag and lead-bearing sludge in the cleaner production of alkali activated cement with high performance and microbial resistivity. *J. Clean. Prod.* **2019**, *220*, 568–580. [\[CrossRef\]](#)

19. Guzmán-Aponte, L.; Mejía de Gutiérrez, R.; Maury-Ramírez, A. Metakaolin-Based Geopolymer with Added TiO₂ particles: Physicomechanical Characteristics. *Coatings* **2017**, *7*, 233. [[CrossRef](#)]
20. Mohd Adnan, M.A.; Muid Julkapli, N.; Amir, M.N.I.; Maamor, A. Effect on different TiO₂ photocatalyst supports on photodecolorization of synthetic dyes: A review. *Int. J. Environ. Sci. Technol.* **2019**, *16*, 547–566. [[CrossRef](#)]
21. Haider, A.J.; Anbari, R.; Kadhim, G.R.; Salame, C.T. Exploring potential environmental applications of TiO₂ nanoparticles. *Energy Procedia* **2017**, *119*, 332–345. [[CrossRef](#)]
22. Hoffmann, M.R.; Martin, S.T.; Choi, W.; Bahnemann, D.W. Environmental Applications of Semiconductor Photocatalysis. *Chem. Rev.* **1995**, *95*, 69–96. [[CrossRef](#)]
23. Mejía, J.M.; Mendoza, J.D.; Yucuma, J.; Mejía de Gutiérrez, R.; Mejía, D.E.; Astudillo, M. Mechanical, in-vitro biological and antimicrobial characterization as an evaluation protocol of a ceramic material based on alkaline activated metakaolin. *Appl. Clay Sci.* **2019**, *178*, 105141. [[CrossRef](#)]
24. Syamsidar, D.; Nurfadilla, S. The Properties of Nano TiO₂ -Geopolymer Composite as a Material for Functional Surface Application. *MATEC Web Conf.* **2017**, *97*, 01013. [[CrossRef](#)]
25. Sikora, P.; Augustyniak, A.; Cendrowski, K.; Horszczaruk, E.; Rucinska, T.; Nawrotek, P.; Mijowska, E. Characterization of mechanical and bactericidal properties of cement mortars containing waste glass aggregate and nanomaterials. *Materials* **2016**, *9*, 701. [[CrossRef](#)] [[PubMed](#)]
26. Hamidi, F.; Aslani, F. TiO₂-based Photocatalytic Cementitious Composites: Materials, Properties, Influential Parameters, and Assessment Techniques. *Nanomaterials* **2019**, *9*, 1444. [[CrossRef](#)] [[PubMed](#)]
27. Sunada, K.; Watanabe, T.; Hashimoto, K. Bactericidal Activity of Copper-Deposited TiO₂ Thin Film under Weak UV Light Illumination. *Environ. Sci. Technol.* **2003**, *37*, 4785–4789. [[CrossRef](#)]
28. Saito, T.; Iwase, T.; Horie, J.; Morioka, T. Mode of photocatalytic bactericidal action of powdered semiconductor TiO₂ on mutants streptococci. *J. Photochem. Photobiol. B* **1992**, *14*, 369–379. [[CrossRef](#)]
29. Oguma, K.; Katayama, H.; Ohgaki, S. Photoreactivation of Escherichia coli after Low- or Medium-Pressure UV Disinfection Determined by an Endonuclease Sensitive Site Assay. *Appl. Environ. Microbiol.* **2002**, *68*, 6029–6035. [[CrossRef](#)]
30. Gogniat, G.; Thyssen, M.; Denis, M.; Pulgarin, C.; Dukan, S. The bactericidal effect of TiO₂ photocatalysis involves adsorption onto catalyst and the loss of membrane integrity. *FEMS Microbiol. Lett.* **2006**, *258*, 18–24. [[CrossRef](#)]
31. Mazurkova, N.A.; Spitsyna, Y.E.; Shikina, N.V.; Ismagilov, Z.R.; Zagrebel'nyi, S.N.; Ryabchikova, E.I. Interaction of titanium dioxide nanoparticles with influenza virus. *Nanotechnol. Russia* **2010**, *5*, 417–420. [[CrossRef](#)]
32. Adams, L.K.; Lyon, D.Y.; McIntosh, A.; Alvarez, P.J.J. Comparative toxicity of nano-scale TiO₂, SiO₂ and ZnO water suspensions. *Water Sci. Technol.* **2006**, *54*, 327–334. [[CrossRef](#)]
33. Armelao, L.; Barreca, D.; Bottaro, G.; Gasparotto, A.; Maccato, C.; Maragno, C.; Tondello, E.; Stangar, U.L.; Bergant, M.; Mahne, D. Photocatalytic and antibacterial activity of TiO₂ and Au/TiO₂ nanosystems. *Nanotechnology* **2007**, *18*, 375709. [[CrossRef](#)]
34. Dědková, K.; Matějová, K.; Lang, J.; Peikertová, P.; Kutláková, K.M.; Neuwirthová, L.; Frydryšek, K.; Kukutschová, J. Antibacterial activity of kaolinite/nanoTiO₂ composites in relation to irradiation time. *J. Photochem. Photobiol. B* **2014**, *135*, 17–22.
35. Gurr, J.R.; Wang, A.S.S.; Chen, C.H. Ultrafine titanium dioxide particles in the absence of photoactivation can induce oxidative damage to human bronchial epithelial cells. *Toxicology* **2005**, *213*, 66–73. [[CrossRef](#)]
36. Hamdany, A.H. Photocatalytic Cementitious Material for Self-Cleaning and Anti-Microbial Application. Ph.D. Thesis, Nanyang Technological University, Singapore, 2019.
37. Davidson, H.; Poon, M.; Saunders, R.; Shapiro, I.M.; Hickok, N.J.; Adams, C.S. Tetracycline tethered to titanium inhibits colonization by Gram-negative bacteria. *J. Biomed. Mater. Res. B Appl. Biomater.* **2015**, *103*, 1381–1389. [[CrossRef](#)]
38. Lorenzetti, M.; Dogša, I.; Stošćki, T.; Stopar, D.; Kalin, M.; Kobe, S.; Novak, S. The Influence of Surface Modification on Bacterial Adhesion to Titanium-Based Substrates. *ACS Appl. Mater. Interfaces* **2015**, *7*, 1644–1651. [[CrossRef](#)] [[PubMed](#)]
39. Peng, Z.; Ni, J.; Zheng, K.; Shen, Y.; Wang, X.; He, G.; Jin, S.; Tang, T. Dual effects and mechanism of TiO₂ nanotube arrays in reducing bacterial colonization and enhancing C3H10T1/2 cell adhesion. *Int. J. Nanomed.* **2013**, *8*, 3093–3105.
40. Daly, M.J.; Gaidamakova, E.K.; Matrosova, V.Y.; Vasilenko, A.; Zhai, M.; Leapman, R.D.; Lai, B.; Ravel, B.; Li, S.-M.W.; Kemner, K.M.; et al. Protein Oxidation Implicated as the Primary Determinant of Bacterial Radioresistance. *PLoS Biol.* **2007**, *5*, 92. [[CrossRef](#)]
41. Carre, G.; Estner, M.; Gies, J.-P.; Andre, P.; Hamon, E.; Ennahar, S.; Keller, V.; Keller, N.; Lett, M.-C.; Horvatovich, P. TiO₂ Photocatalysis Damages Lipids and Proteins in Escherichia coli. *Appl. Environ. Microbiol.* **2014**, *80*, 2573–2581. [[CrossRef](#)] [[PubMed](#)]
42. Kubacka, A.; Diez, M.S.; Rojo, D.; Bargiela, R.; Ciordia, S.; Zapico, I.; Albar, J.P.; Barbas, C.; Martins dos Santos, V.A.P.; Fernández-garcía, M.; et al. Understanding the antimicrobial mechanism of TiO₂-based nanocomposite films in a pathogenic bacterium. *Sci. Rep.* **2014**, *4*, 4134. [[CrossRef](#)] [[PubMed](#)]
43. Mejía-de Gutiérrez, R.; Villaquirán-Cacedo, M.; Ramírez-Benavides, S.; Astudillo, M.; Mejía, D. Evaluation of the Antibacterial Activity of a Geopolymer Mortar based on Supplemented with TiO₂ and CuO Particles Using Glass Waste as Fine Aggregate. *Coatings* **2020**, *10*, 157. [[CrossRef](#)]
44. Pacheco-Torgal, F.; Jalali, S. Nanotechnology: Advantages and drawbacks in the field of construction and building materials. *Contr. Build. Mater.* **2011**, *25*, 582–590. [[CrossRef](#)]

45. Cho, M.; Chung, H.; Choi, W.; Yoon, J. Linear correlation between inactivation of *E. coli* and OH radical concentration in TiO₂ photocatalytic disinfection. *Water Res.* **2004**, *38*, 1069–1077. [[CrossRef](#)]
46. Janus, M.; Zajac, K. Concretes with Photocatalytic Activity. In *High Performance Concrete Technology and Applications*; Yilmax, S., Baytan, H., Eds.; IntechOpen: London, UK, 2016; Chapter 7, pp. 141–161.
47. Carmona-Quiroga, P.M.; Martinez-Ramirez, S.; Viles, H.A. Efficiency and durability of a self-cleaning coating on concrete and stones under both natural and artificial ageing trials. *App. Surf. Sci.* **2018**, *433*, 312–320. [[CrossRef](#)]
48. Grebenișan, E.; Hegyi, A.; Szilagyi, H.; Lăzărescu, A.V.; Ionescu, B.A. Influence of the Addition of TiO₂ Nanoparticles on the Self-Cleaning Performance of Cementitious Composite Surfaces. *Proceedings* **2020**, *1*, 42. [[CrossRef](#)]
49. Grebenișan, E.; Hegyi, A.; Lăzărescu, A.V. Research Regarding the Influence of TiO₂ Nanoparticles on the Performance of Cementitious Materials. In *IOP Conference Series: Materials Science and Engineering, Proceedings of the International Conference on Innovative Research—ICIR EUROINVENT 2020, Iasi, Romania, 21–23 May 2020*; IOP Publishing: Bristol, UK, 2020; Volume 877, p. 012004.
50. Hegyi, A.; Szilagyi, H.; Grebenișan, E.; Sandu, A.V.; Lăzărescu, A.V.; Romila, C. Influence of TiO₂ Nanoparticles Addition on the Hydrophilicity of Cementitious Composites Surfaces. *Appl. Sci.* **2020**, *10*, 4501. [[CrossRef](#)]
51. Gopalan, A.-I.; Lee, J.-C.; Saianand, G.; Lee, K.-P.; Sonar, P.; Dharmarajan, R.; Hou, Y.; Ann, K.-Y.; Kannan, V.; Kim, W.-J. Recent progress in the abatement of hazardous pollutants using photocatalytic TiO₂-based building materials. *Nanomaterials* **2020**, *10*, 1854. [[CrossRef](#)]
52. Shaaban, I.G.; El-Sayad, H.; El-Ghaly, A.E.; Moussa, S. Effect of micro TiO₂ on cement mortar. *EJME* **2020**, *5*, 58–68. [[CrossRef](#)]
53. Daniyal, M.; Azam, A.; Akhtar, S. Application of Nanomaterials in Civil Engineering. In *Nanomaterials and Their Applications. Advanced Structured Materials*; Khan, Z., Ed.; Springer: Singapore, 2018; Volume 84, pp. 169–189.
54. Wang, D.; Geng, Z.; Hou, P.; Yang, P.; Cheng, X.; Huang, S. Rhodamine B Removal of TiO₂@ SiO₂ Core-Shell Nanocomposites Coated to Buildings. *Crystals* **2020**, *10*, 80. [[CrossRef](#)]
55. Guo, M.Z.; Maury-Ramirez, A.; Poon, C.S. Self-cleaning ability of titanium dioxide clear paint coated architectural mortar and its potential in field application. *J. Clean. Prod.* **2016**, *112*, 3583–3588. [[CrossRef](#)]
56. Sikora, P.; Cendrowski, K.; Markowska-Szczupak, A.; Horszczaruk, E.; Mijowska, E. The effects of silica/titania nanocomposite on the mechanical and bactericidal properties of cement mortars. *Constr. Build. Mater.* **2017**, *150*, 738–746. [[CrossRef](#)]